ADVANCED HEALTHCARE MATERIALS
www.advhealthmat.de

Skin Conformal Polymer Electrodes for Clinical ECG and EEG Recordings

*Flurin Stauffer, Moritz Thielen, Christina Sauter, Séverine Chardonnens, Simon Bachmann, Klas Tybrandt, Christian Peters, Christofer Hierold, and Janos Vörös**

Preparation-free and skin compliant biopotential electrodes with high recording quality enable wearables for future healthcare and the Internet of Humans. Here, super-soft and self-adhesive electrodes are presented for use on dry and hairy skin without skin preparation or attachment pressure. The electrodes show a skin-contact impedance of 50 kΩ cm^2 at 10 Hz that is comparable to clinical standard gel electrodes and lower than existing dry electrodes. Microstructured electrodes inspired by grasshopper feet adhere repeatedly to the skin with a force of up to 0.1 N cm^{-2} without further attachment even during strong movement or deformation of the skin. Skin compliance and adhesive properties of the electrodes result in reduction of noise and motion artifacts superior to other dry electrodes reaching the performance of commercial gel electrodes. The signal quality is demonstrated by recording a high-fidelity electrocardiograms of a swimmer in water. Furthermore, an electrode with soft macropillars is used to detect alpha activity in the electroencephalograms from the back of the head through dense hair. Compared to gel electrodes, the soft biopotential electrodes are nearly imperceptible to the wearer and cause no skin irritations even after hours of application. The electrodes presented here could combine unobtrusive and long-term biopotential recordings with clinical-grade signal performance.

1. Introduction

Long-term recording of human biopotentials allows for early detection, diagnosis, and recovery monitoring of a large number of brain-, heart-, and muscle-related diseases.[1] Preparation-free biopotential electrodes are a central element of wearable devices for future health care and the Internet of Humans. Current clinical standard electrolyte gel electrodes have limited long-term recording capabilities due to a lack of comfort, possible skin irritation, and long-term stability issues. Recently emerging dry electrodes have been shown to improve comfort, wear time, and a reduction of skin irritation.[2,3] However, most of these approaches still lack the recording quality required for medical diagnostics. Dry electrodes based on soft polymers are especially of interest since they can conform to the rough skin and adapt to its movements. Therefore, they provide a tight electrode-skin contact that can improve performance by reducing motion artifacts and increasing signal-to-noise ratio (SNR).[2] Electrically conductive electrodes based on soft polymers can be achieved by patterning of mesh-like metal structures on the surface[4,5] or by mixing with conductive fillers such as metallic or carbon particles,[6–9] nanotubes,[10] or nanowires.[11] Biopotentials were successfully recorded using all approaches but showed high skin-contact impedances compared to standard gel electrodes. A higher skin-contact impedance leads to an increased impedance mismatch that reduces common mode rejection and therefore the SNR.[12] A strategy to decrease and control the impedance is a fluid reservoir integrated with the electrode.[13] Fixation and user comfort are key aspects to consider in addition to the electrical properties of the electrodes. Clinical electrodes are usually fixed with medical skin adhesives based on acrylic or silicone formulations. The main adhesion forces are covalent bonds and Van der Waals interactions. Self-adhesive electrodes can be obtained by using extra soft or microstructured polymers.[5,10,14] Such micropillar geometries are inspired by nature of the gecko and grasshopper feet.[15] The main mechanism of the adhesion are Van der Waals interactions between the pillar tip and the surface.[16] Bae et al. used such microstructures to create a self-adhesive patch for fixation of a conventional gel electrode.[17] Kim et al. created an electrode that combines adhesive and electric properties to one patch and demonstrated proof-of-principle electrocardiogram (ECG) measurements.[14] However, the required electrode area of about 25 cm^2 seems too large for practical biopotential measurements. This is probably due to the comparably low electrical conductivity of the carbon-based composite (0.01 S cm^{-1}) and resulting high electrode-skin impedances.

In this work, we present soft and self-adhesive micropillar electrodes with drastically decreased electrode-skin impedance to record biopotentials with clinical quality. The electrodes were fabricated using a novel process that is time and cost-efficient as well as upscalable. We characterized the electrode performance

F. Stauffer, S. Bachmann, Prof. K. Tybrandt, Prof. J. Vörös
Laboratory of Biosensors and Bioelectronics
ETH Zurich
Gloriastrasse 35, 8092 Zürich, Switzerland
E-mail: janos.voros@biomed.ee.ethz.ch
M. Thielen, C. Sauter, S. Chardonnens, Dr. C. Peters, Prof. C. Hierold
Micro and Nanosystems
ETH Zurich
Tannenstrasse 3, 8092 Zürich, Switzerland

DOI: 10.1002/adhm.201700994

by a detailed investigation of the impedance and the susceptibility for artifacts in direct comparison to standard wet electrodes. We achieved similar performance in both aspects allowing for high resolution recordings without using gels or causing irritation upon long-term wear. As a proof-of-principle for challenging user scenarios, we successfully recorded ECG underwater even while swimming. Finally, we demonstrated that our soft electrodes can comfortably monitor electroencephalograms (EEG) through dense hair using a macropillar design.

2. Results and Discussions

The developed soft epidermal electrodes are of clinically relevant size and comprise of a soft conductive base with specific coatings and surface structures. The silicone rubbers were loaded with conductive silver particles to achieve a stretchable composite material with high electrical conductivity of >100 S cm^{-1}.[18] The composite was molded into different shapes and coated as shown in **Figure 1**A–C and described in the Experimental Section. The use of soft materials has several advantages compared to rigid devices. If the elastic modulus of the electrode is similar to that of the epidermis the electrode can move and deform together with the skin. This makes it imperceptible to the wearer and can reduce relative movement between the electrode and the skin creating a more stable interface. Also, the soft polymer might compensate for micro- and nanoroughness of the skin, increasing the skin-contact area. If the electrode surface is additionally rough or even porous,

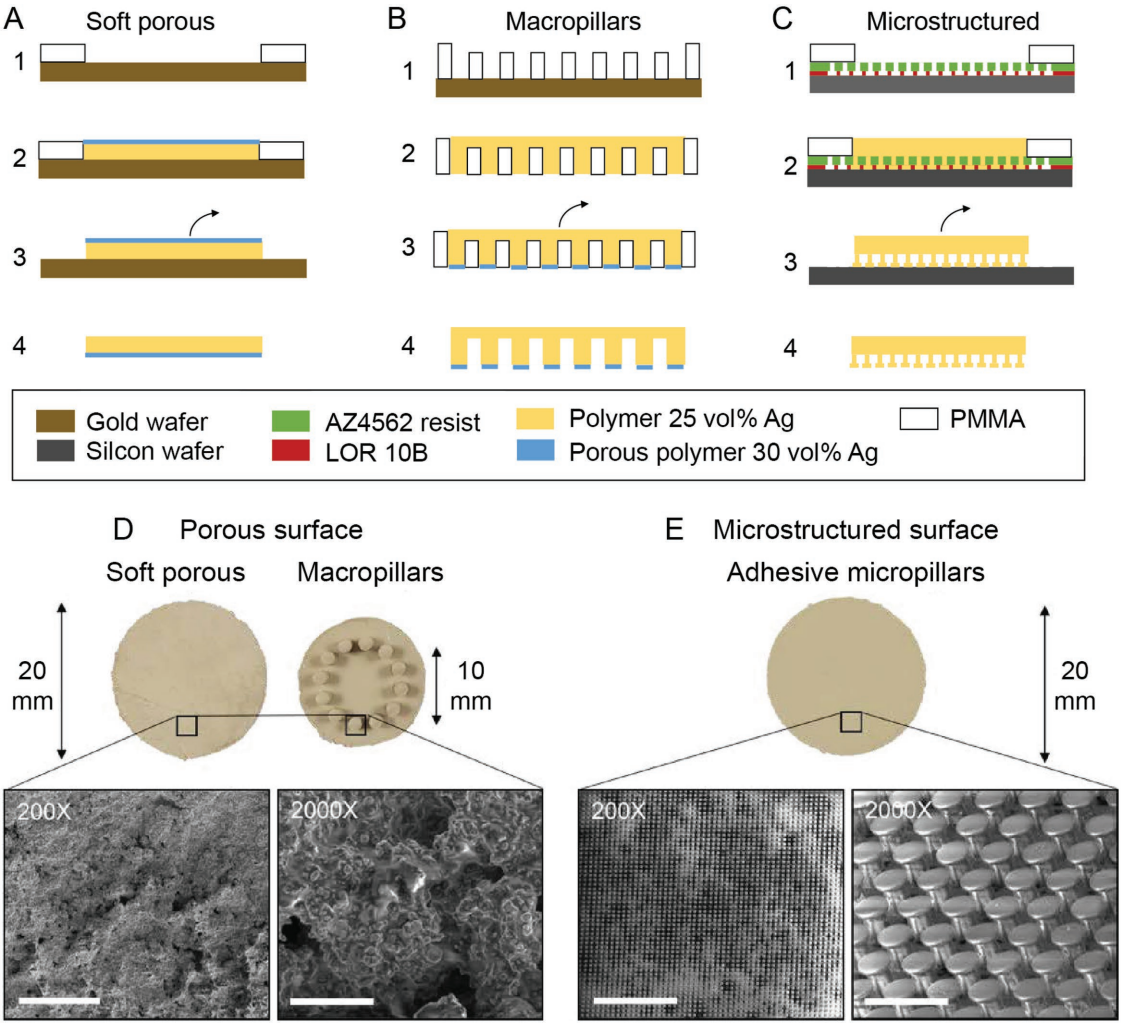

Figure 1. Soft epidermal electrodes for biopotential recordings. Fabrication process of A) soft porous electrodes. A1) Laser-cut poly(methyl methacrylate) (PMMA) stencil mask on top of a gold wafer defines the geometry of the electrode, A2) first conductive polymer (25 vol% Ag) and second highly conductive porous polymer (30 vol% Ag) is stencil printed, A3) the mask is removed, and A4) the electrode is peeled from the substrate. B) Macropillar electrodes. B1) PMMA is used as mask for macropillars and base, A2) conductive polymer is printed into the mold, A3) the screen is removed, and A4) the electrode is peeled off. C) Microstructured electrodes. C1) Lift off resist (LOR) and photoresist (PR) are spincoated on a silicon substrate and then structured by photolithography. The photoresist defines the micropillar geometry, the LOR the size of the pillar-tips. PMMA is used as a screen. C2) Conductive polymer is printed into the mold, C3) the screen is removed and LOR and PR are dissolved in Acetone causing, and C4) the release of the electrode. D) Soft electrodes with porous surface without pillars for high comfort and good electrical properties (electrode thickness = 100 µm) and with soft macropillarsfor the application through dense hair (base thickness = 500 µm, pillar height = 2 mm, pillar diameter = 1 mm). E) Soft electrode with grasshopper inspired microstructured surface for improved dry adhesion to the skin (thickness = 100 µm). The scale bars are 200 µm (200×) and 20 µm (2000×).

the electrochemically active area can be enlarged resulting in decreased electrode-skin impedance.

We combined a soft conductive base with a porous and highly conductive coating on the electrodes shown in Figure 1D. Silver microparticles with an average diameter of 2–3.5 µm (AgLMP) were used as conductive filler. For the application on most body surfaces, we designed a 100 µm thin circular electrode with a diameter of 20 mm. The small area of 3.14 cm^2 allows for biopotential recordings with high spatial resolution. The elastic modulus of ≈1 MPa is similar to the one of the human skin resulting in full compliance (Figure S1, Supporting Information). The surface in contact with the skin is covered by a soft and highly conductive porous layer of ≈2 µm thickness as shown in the scanning electron microscope (SEM) image insets. For body areas covered by dense hair such as the head, we shaped the same material combination into macroscopic pillars as shown in Figure 1D. The macropillar electrode consists of a conductive base of 15 mm diameter and 12 soft pillars (d = 1 mm, h = 2 mm, pitch = 10 mm) that allow contacting the scalp even through dense hair. The pillars and small area of 1.77 cm^2 make this electrode suitable for high resolution EEG recordings. EEG signals are a magnitude smaller than ECG or electromyograms (EMG) and therefore require a low skin-contact impedance for successful high-quality signal readout. This is a major challenge considering the small contact areas available for clinical EEG.

Additional functionality of the electrodes was achieved by microstructuring of the surface as shown in Figure 1E. The electrodes are inspired by grasshopper feet and can adhere to arbitrary surfaces by enhanced Van der Waals interaction. The microstructures have a pillar shaped base with a flat tip with geometries that can compensate for microscopic grooves in the epidermis, which has an rms roughness around 10–30 µm.[19] The base pillar has a height of 10 µm and a diameter of 5 µm. The tip diameter is 7–8 µm and the height is 2 µm. The pitch of the structures is 12 µm for dense surface coverage without pillars sticking together. As the tip height is only 2 µm, we compared electrodes with large (AgLMP = 2–3.5 µm) with small filler particles (AgSMP = 0.5–1 µm) as they differ on how they fill the tips. With these dimensions, the soft electrode base in combination with the microstructures enable a conformal contact to the micro- and macroscopic topography of the skin surface. The selected aspect ratio of 2:1 provides a good tradeoff between adhesion performance, skin conformity, and fabrication yield. Higher aspect ratios above 3:1 lead to a collapse of the soft pillars (Figure S2, Supporting Information).[14] Upon collapsing, the adhesive properties are mostly lost. The increase in adhesion properties by using pillars can be explained by the principle of contact splitting, as delamination is less dependent on crack propagation at the electrode-skin interface.[20] For flat pillars, this leads to an increase in pull off force by $P_c' = n^{1/4} P_c$ with n equals number of pillars.[16] The mushroom shape further minimizes stress at the edges of the structure during pull-off, diminishing crack propagation.[21] Therefore, the soft micropillars can potentially reduce motion artifacts by compensating the relative movement between skin and the electrode base. The electrodes are almost imperceptible to the wearer and nicely match movement and deformation (Video S1, Supporting Information). This electrode is well suited for ECG or EMG applications where tight contact between skin and electrode is required.

To assess the electrode-skin impedance, a three-electrode setup was used, as shown in **Figure 2**A, with the electrode under test (working electrode: WE) and standard gel electrodes

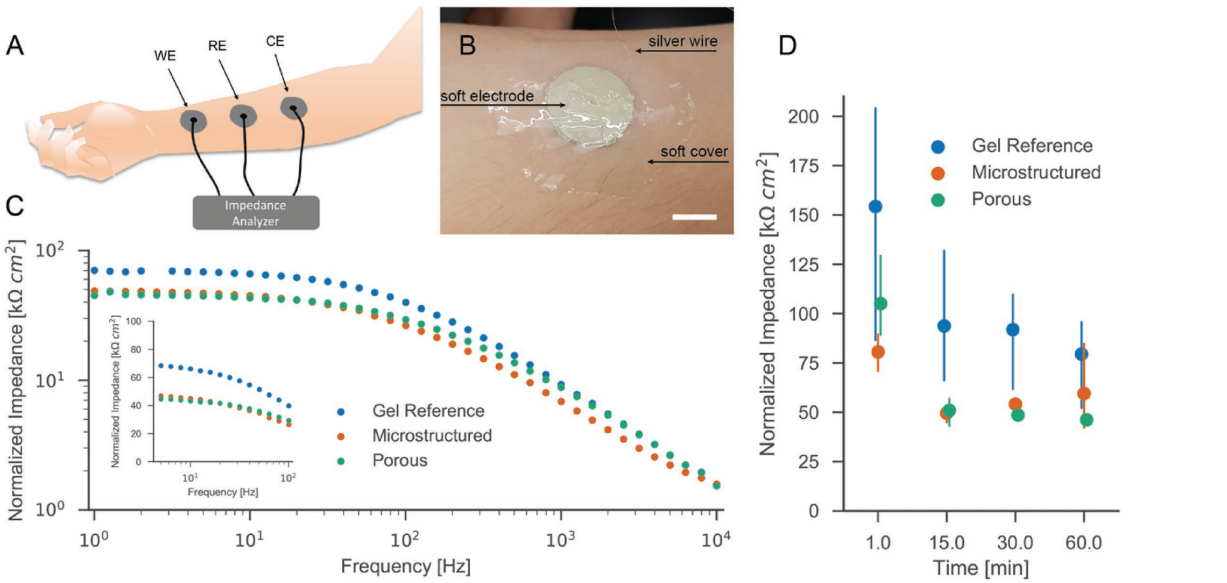

Figure 2. Characterization of the electrode-skin impedance without skin preparation or attachment pressure. A) Impedance measurement configuration. B) Soft polymer electrode mounted on the skin. Electrical contact is established with a thin silver wire on the upper surface of the electrode. Electrode and wire are covered with a 100 µm thick Ecoflex sheet that ensures stable electrical contact and flexible mounting (scale bar is 1 cm). C) Frequency dependence of normalized electrode-skin impedance comparing porous and microstructured polymer electrodes to standard gel electrodes after 15 min of wear time. The inset shows a magnification of the frequency range relevant for biopotential recordings with linear y-axis. D) Impedance values at 10 Hz over time during the first hour of wear time presented as mean with estimated 95% confidence interval (n = 3).

as reference electrode (RE) and counter electrode (CE). The soft polymer electrode placed on the skin was electrically connected with a thin silver wire on the electrode backside and held in place by a 100 µm thin Ecoflex patch covering the electrode and surrounding skin as shown in Figure 2B. The electrode-skin impedance (normalized by the projected area, $Z_{norm} = Z_{meas} \times A_{electrode}$) of the different electrode types is shown in Figure 2C 15 min after attachment on the skin without pressure or skin preparation. The corresponding phase is similar in all electrode types and is shown in Figure S3 (Supporting Information). The characterized soft porous electrodes contain AgLMP and the microstructured electrodes AgSMP as described in Figure 1. Because the skin-contact impedance is highly dependent on the subject, skin condition, and environmental factors, we used commercial gel patch electrodes for comparison. In the relevant frequency ranges up to 100 Hz (Figure 2C, inset), the two polymer electrode types performed better than the gel reference. At 10 Hz the porous electrode showed a contact impedance of 43 kΩ cm^2 (13.6 kΩ per electrode) and the microstructured electrode of 45 kΩ cm^2 (14.3 kΩ per electrode). The gel electrode had a contact impedance of 66 kΩ cm^2 (24.4 kΩ per electrode). The performance of porous electrodes could potentially be further improved by increasing the porosity using smaller filler particles. The impedance variation at 10 Hz during the first hour of attachment is shown in Figure 2D. Three electrodes of each type were tested on the same person, location, and day. All electrodes showed a higher initial impedance before the interface stabilized after 15 min. During 1 h, the mean impedance reduced from 154.3 ± 49.6 to 79.5 ± 19.4 kΩ cm^2 for gel, from 80.6 ± 7.6 to 59.5 ± 18.2 kΩ cm^2 for microstructured, and from 105.1 ± 17.4 to 46.2 ± 1.9 kΩ cm^2 for soft porous electrodes. Gel electrodes showed a higher mean skin-contact impedance and variation compared to the soft polymer electrodes throughout the measurements. However, using the two-sample Welsh's *t*-test we have found no significant differences for a confidence interval of 0.05.

The self-adhesive properties and relation to skin impedance of the different electrode types are shown in **Figure 3**. A self-adhesive soft microstructured electrode attached to the skin of the forearm is shown in Figure 3-A1. A thin silver wire is attached to the electrode using a thin Ecoflex cover (cover partially removed in the image). Using tweezers, we applied a strong lateral force on the electrode that caused similar movement of the underlying skin without delamination of the electrode as shown in Figure 3-A2. On glass, the lateral adhesion force was so high that the sample deformed and ruptured without delamination (Figure S4, Supporting Information). Peeling of the electrode from the skin could be done by applying a perpendicular pulling force as demonstrated in Figure 3-A3 and the electrode did not leave any visible mark as shown in Figure 3-A4. Even after 10 h of wear time, no skin irritation was observed as shown in Figure S5 (Supporting Information). In comparison, the skin was clearly irritated for gel patch electrodes.

The adhesion to the skin for a perpendicular force is shown in Figure 3B for electrodes already used repeatedly. For each electrode type, two samples were attached and detached subsequently for 10 times. Electrodes with porous coating (flat and macropillars) adhered with a mean force of 15.7 ± 1.9 mN cm^{-2} on the skin. The low adhesion was likely caused by a low contact area between skin and polymer surface of the electrode. The microstructured electrodes showed significantly higher adhesion forces of 38.7 ± 5.5 mN cm^{-2} for small microparticles (AgSMP, 0.5–1 µm) and of 103.3 ± 11.6 mN cm^{-2} for large microparticles (AgLMP, 2–3.5 µm) as conductive filler. These values are somewhat lower than other reports on adhesive micropillars since we measured on real skin with hairs, without skin preparation and after repeated use. Initial adhesion values for the first use were up to seven times higher (Figure S6, Supporting Information). The use of smaller silver particles resulted in a rough pillar tip interface reducing contact area and adhesion (116 mN per electrode). With larger particles as conductive fillers, the surface of the pillars was smoother increasing the adhesion force to 309 mN. The microstructures were mechanically robust and showed no damage on the pillar structures, nor any signs of pillar collapsing even after frequent testing (>20× repeated attachment, Figure 3C. The size of filler particles also affected the contact impedance as shown in Figure 3D. Because the microstructured mold has features smaller than the diameter of AgLMP, the effective filler content and therefore the conductivity in the tip of the micropillars was locally reduced. In contrast, smaller filler particles completely fill the tips of the microstructured pillars. Therefore, a tradeoff between mechanical adhesion and contact impedance must be considered when choosing application specific electrode parameters.

We compared the susceptibility of different electrode types (gel = blue, porous = green, microstructured = orange) to signal noise and motion artifacts as shown in **Figure 4**. Motion artifacts in a real-life scenario originate from different and often non-reproducible effects. To facilitate the comparison of electrode types in a reproducible way we used an experimental setup (Figure S7, Supporting Information) to induce strong relative motion of electrode and skin while retaining a defined attachment pressure. First, we simultaneously measured differential biopotentials between the electrode under test and one gel electrode on the same and on the opposite arm without movement of the wearer (Figure 4A). This configuration allowed to obtain the signal noise (Figure 4B) and the ECG (Figure 4D) at the same time. While the subject was in rest, all electrodes placed on the same arm produced a flat noise signal with low baseline drift that can be filtered since it is below 0.5 Hz without influencing the ECG recordings (Figure 4B). From a visual inspection of the signal, artifacts, and drift were similar in all electrodes. This was also reflected in the analysis of the RMS noise of the filtered signal (bandpass: 0.5–120 Hz, notch: 50 Hz) shown in Figure 4C. The mean noise of porous electrodes was slightly higher, the microstructured slightly lower compared to the gel electrodes. However, the differences were not statistically significant.

We performed the same analysis on the ECG signal shown in Figure 4D. When measuring between the two forearms, all electrodes recorded a high-fidelity ECG with all elements of the PQRST waveform clearly visible. The SNR of the ECG signal, shown in Figure 4E, was obtained from the bandpower (integral of the power spectral density) divided by the bandpower of the noise

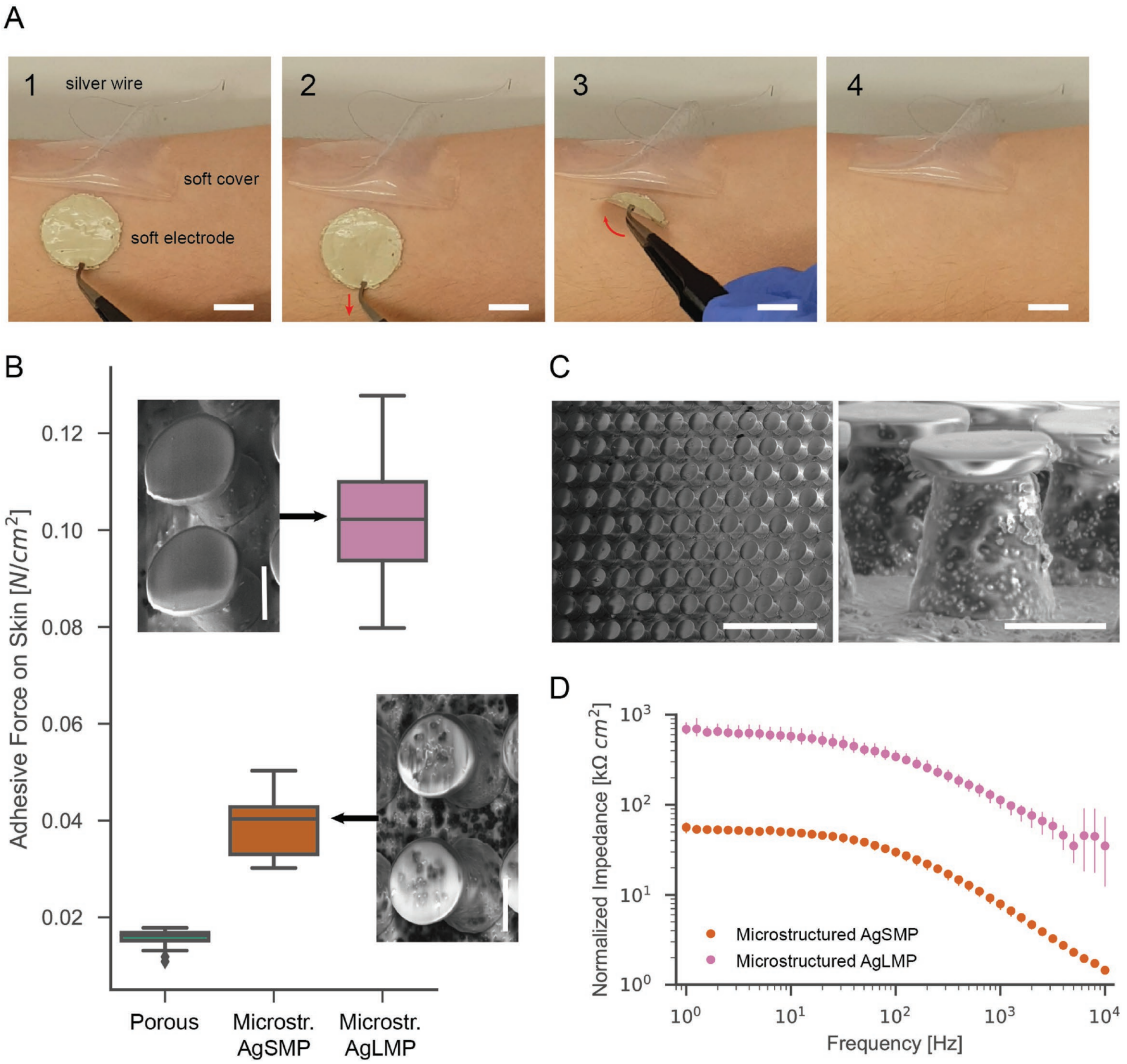

Figure 3. Skin adhesion properties of soft electrodes. A1) Soft microstructure electrode on the skin with partially removed Ecoflex cover and silver wire (scale bars are 1 cm). A2) Strong horizontal force on the electrode also moves the skin without delamination. A3) Peeling of the electrode can be done by applying a perpendicular pulling force. A4) The electrode leaves no visible mark on the skin. B) Perpendicular adhesion force on the skin of the forearm for the polymer electrodes with porous coating, microstructures with small (AgSMP), and large (AgLMP) microparticles. Values are measured after repeated use (>5 times and >1 h wear time, 20 repeats, $n = 2$). The skin was not pretreated and was slightly hairy. The insets show two micropillars containing AgSMP and AgLMP (scale bar is 5 µm). C) Microstructures showed no sign of damage after >20x use and cleaning with ethanol (scale bars are 40 and 5 µm). D) Normalized electrode-skin impedance over frequency comparing microstructured polymer electrodes with AgSMP and AgLMP presented as mean with estimated 95% confidence interval ($n = 3$).

signal. Microstructured electrodes showed the highest mean SNR but all tested electrodes performed equally within error.

We then subjected the electrodes to repeated strong uniaxial movement of 1.4 cm and 2 Hz with an actively controlled pressure as shown in Figure 4F. This is a higher displacement than expected even during high activity applications. The forearm signal in Figure 4G was a direct representation of the movement induced artifacts. The artifacts were clearly visible for all electrodes with similar movement susceptibility. This demonstrates that skin conformity can compensate the external movement to some extend by transferring the force directly to the skin instead of sliding across. The microstructured electrode also prevents sliding motion by adhering to the skin but the length of the micropillars is not sufficient to compensate for the large movement imposed in this study. Compared to the subject in rest, the RMS was increased by a factor of ≈5 as shown in Figure 4H.

Strong movement during the recording of the ECG resulted in a distortion of the QRS complex in all recordings as shown in Figure 4I. Nevertheless, the waveform is reproduced in a satisfactory level that allows for medical evaluation. Within error, all tested electrodes rejected noise similarly well as shown in Figure 4J. Compared to the stationary case, the SNR is reduced by a factor of ≈10.

Because the electrolyte gel compensates for relative movement of body and electrode, wet electrodes usually show superior performance in respect to motion artifacts compared to dry electrodes. We demonstrated that soft and self-adhesive skin

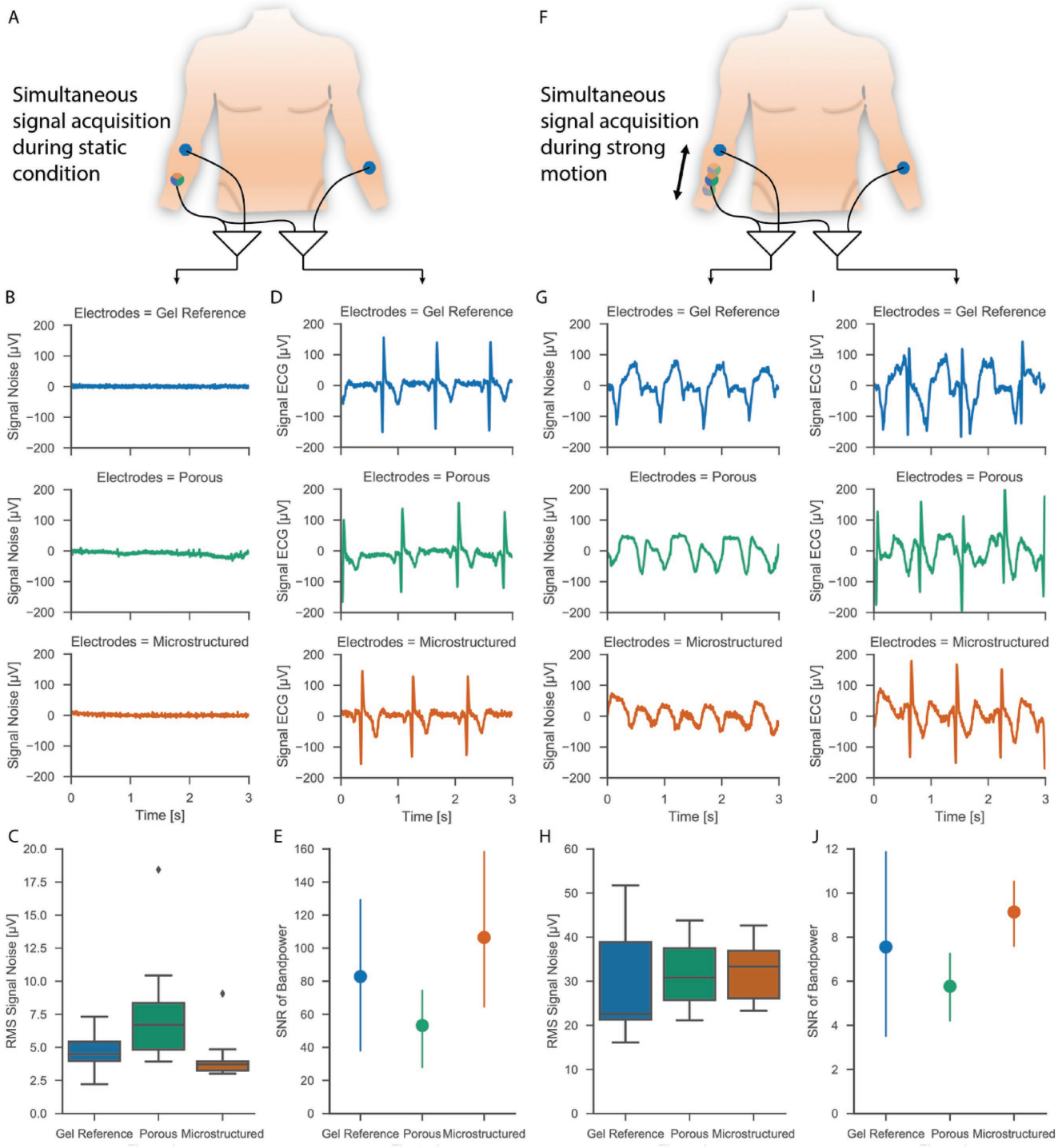

Figure 4. Investigations on noise and movement artifacts during biopotential monitoring for different electrode types. A) Differential biopotentials between the electrode under test (blue/green/orange) were measured simultaneously on the same arm (signal noise) and the opposite arm (ECG signal) without movement. B) Recorded noise signal comparing soft porous and microstructured polymer electrodes with gel electrodes. C) RMS signal noise showed similar performance of all electrodes. D) Comparison of ECG signal in rest. All electrodes reproduced the PQRST waveform. E) Microstructured electrodes showed the highest mean SNR but differences were not significant. F) Unidirectional relative movement of 1.4 cm was applied between the electrode under test and the arm resting on a movable platform while regulating the attachment pressure. G) The motion induced artifacts were clearly visible in all electrodes. H) Analysis of the signal showed similar performance for all electrodes. I) The strong motion distorted the ECG waveform but still allowed to clearly distinguish the QRS waveform. J) All electrodes performed similarly under induced motion. SNR data are presented as mean with estimated 95% confidence interval ($n = 3$). RMS noise was calculated from 15 signal intervals (4 s each) and $n = 3$.

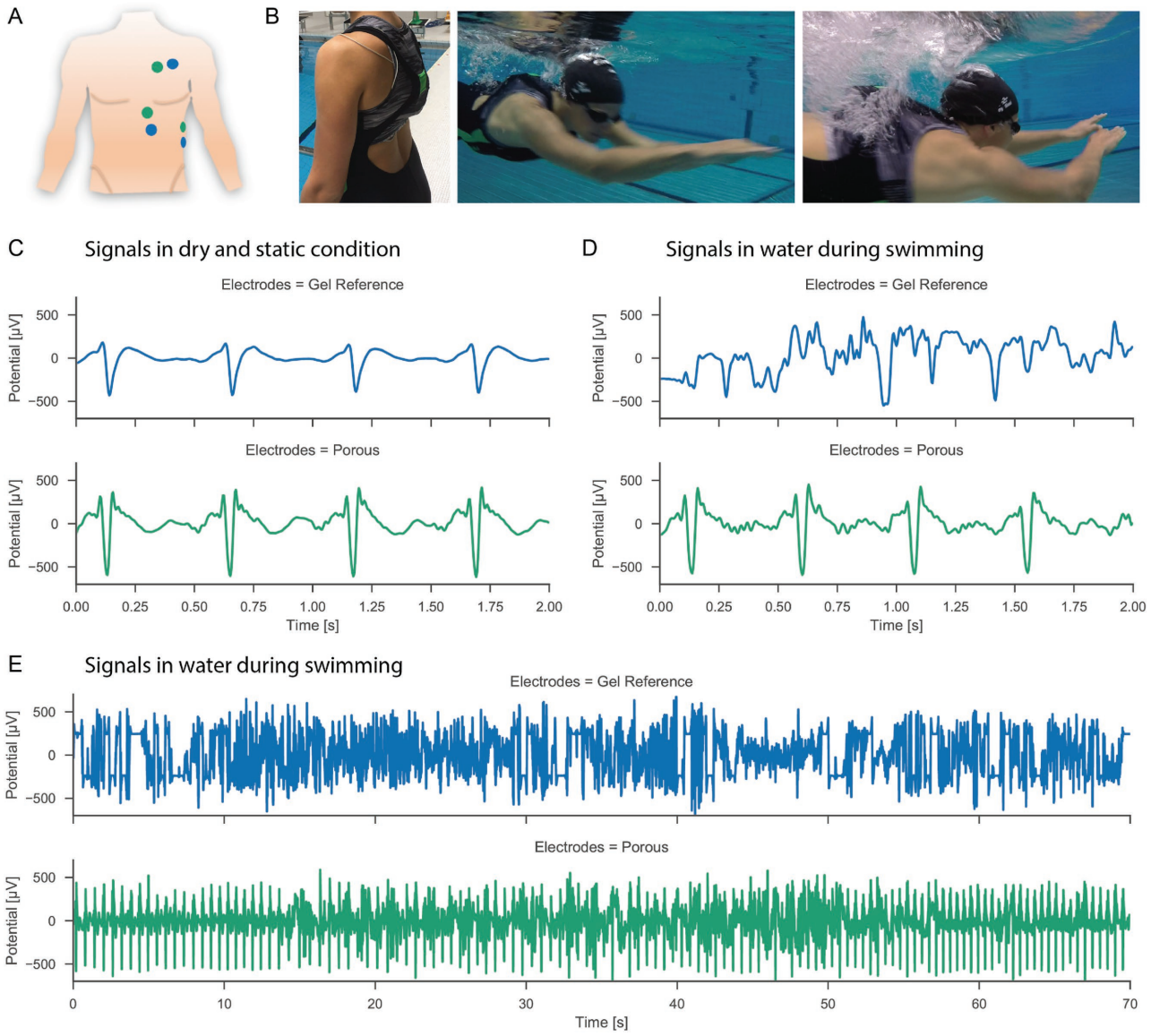

Figure 5. ECG recordings during swimming. A) Electrode placement of the soft polymer electrodes (green) and the gel reference electrodes (blue). B) Fixation of the recording device using textiles and the swimmer in action under water. C) Simultaneous ECG measurements in dry and static condition before swimming for both electrode types. The signals were slightly different due to the placement of the electrodes. D) ECG recordings during swimming showed good signal quality with few small movement artifacts for soft polymer electrodes, whereas the ECG signal with gel electrodes was highly unstable and the ECG amplitudes are not distinguishable from the artifacts. E) ECG recordings for 70 s while swimming lanes with breaststrokes.

compliant dry electrodes can achieve similar performance even under strong induced motion.

To demonstrate the potential of the soft electrodes in a challenging usage scenario, ECG were recorded during swimming. This scenario combines strong movements, muscle activity, and a challenging environment. We recorded the ECG of a professional swimmer during training doing breaststroke in the water comparing soft porous electrodes and standard gel patch electrodes. **Figure 5**A shows the placement of the polymer electrodes (green) and of the gel electrodes (blue). The recording electronics were kept in a watertight box on the back and is worn with the electrodes under the swimsuit to not restrain the swim training as shown in Figure 5B. ECG signal of both electrode types before the swimmer entered the water is shown in Figure 5C. The ECG signal was clearly visible with little noise for both electrode types. Differences in the ECG waveform originated from the slightly different placement of the electrodes on the torso. The swimmer then entered the water and started her workout. A short ECG interval while the swimmer was moving underwater is shown in Figure 5D. Motion artifacts were strongly pronounced in the gel electrodes and distorted the ECG signal to an extend that prevents medical diagnostics. The electrolyte gel might dissolve in the chlorinated water and deteriorate long-term stability. In contrast, the porous polymer electrodes showed a meaningful ECG with very little movement noise. This is not a temporary characteristic but occurred while

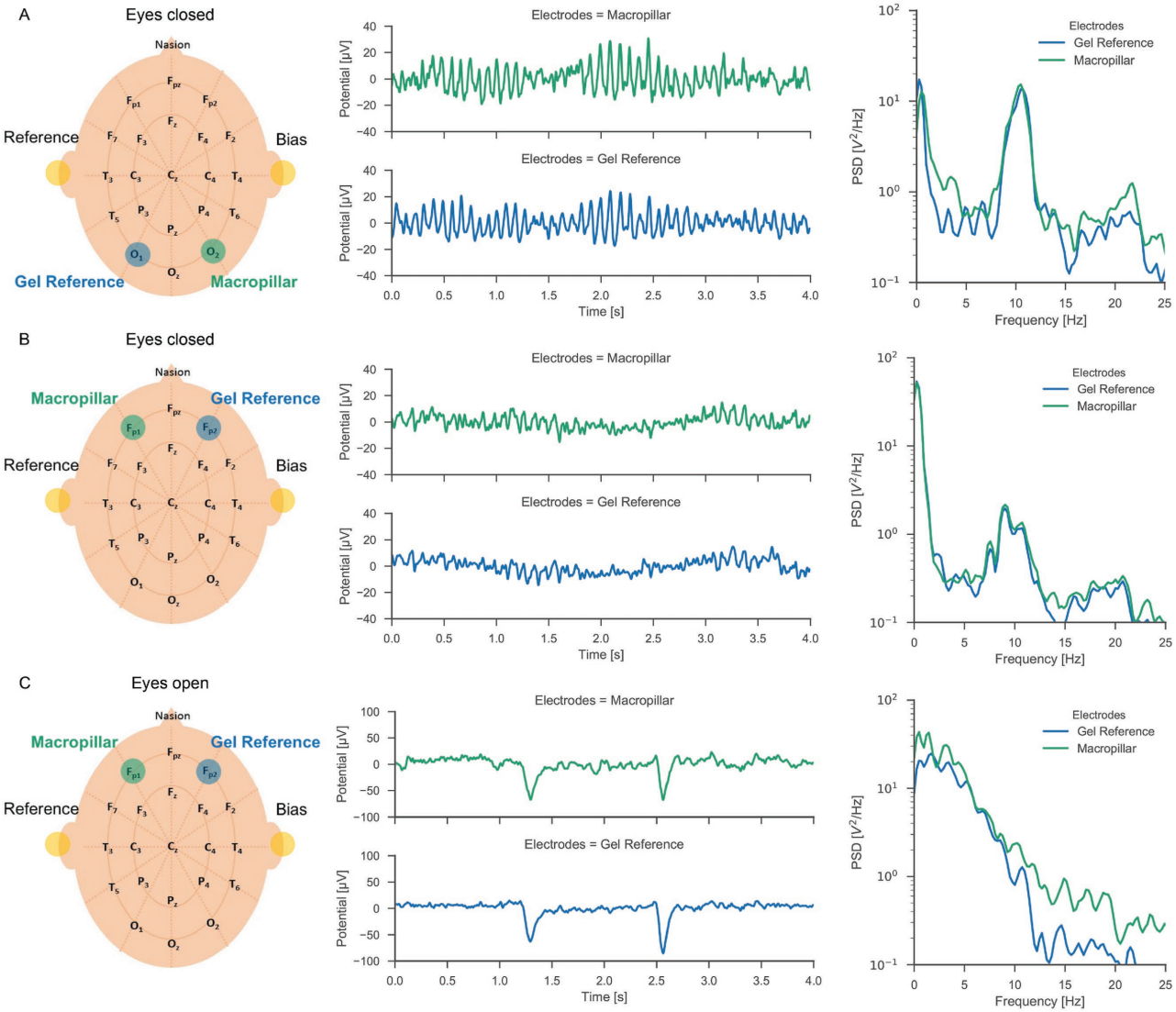

Figure 6. Proof-of-principle EEG measurements using soft pillar electrodes. A) Occipital EEG signals are measured through hair with soft pillar electrodes and clinical standard wet electrodes simultaneously with eyes closed. The power spectral density shows the characteristic alpha wave peak around 10 Hz. B) Alpha waves could also be detected from the forehead when the eyes were closed. C) The alpha waves disappear when the eyes are kept open. The peaks in the time signal correspond to typical eye blink effects.

crossing the full swimlane as shown in Figure 5E. The soft electrode performance allowed a stable signal acquisition even during strong motions, as shown Figure 4. Furthermore, the hydrophobic Ecoflex cover insulates the electrode-skin interface from surrounding liquid.

Recording of an EEG is probably the most challenging test for noninvasive biopotential electrodes due to the low signal amplitudes in the μV range and the dense coverage of the skin by hair. We used our soft macropillar polymer electrodes to detect alpha wave activity from the occipital positions in comparison to clinical standard gold cup electrodes as shown in **Figure 6**A. The electrodes were placed according to the 10–20 system at the back of the head of a male subject with dense hair. The clinical standard electrode was located at O1, the polymer pillar electrode at O2, reference and bias were placed at the earlobes using gold cup electrodes (Figure S8, Supporting Information). The subject was stationary with the eyes closed and tried to relax. The recordings in the time and frequency domain showed a matching EEG for both electrodes and revealed a clear 10 Hz peak that is characteristic for alpha waves. We repeated the EEG measurements at a frontal position located at FP1 and FP2 as shown in Figure 6B. This position might be of higher interest for simple consumer applications and brain computer interfaces. Due to the position on the head, the alpha peak was less pronounced but still clearly visible in both channels. Finally, when the subject opened the eyes the alpha peak disappeared as shown in Figure 6C. Instead, characteristic eye blinking artifacts were observed in the time domain. During 1 h of measurement the subject did not experience any discomfort caused by the soft polymer electrodes. This represents a major advantage over existing rigid dry electrodes. In conclusion, the soft macropillar electrodes showed promising

performance and could enable clinical quality EEG recordings without tedious skin preparation.

3. Conclusion

We presented self-adhesive, soft, and skin conformable biopotential electrodes that can be applied without skin preparation or attachment pressure. Due to the low skin-contact impedance and susceptibility for motion artifacts, the electrodes can acquire high quality biopotentials from small areas even in difficult usage scenarios where the wearer is actively in motion. We demonstrated this by recording of a high-fidelity ECG of a professional swimmer during training in water. We further used an electrode with soft macroscopic pillars to record EEG from the forehead and the back of the head through hair and detected characteristic alpha waves. During characterization and application, the soft polymer electrodes performed equally well or better than commercial standard electrodes. In contrast to gel electrodes, no skin irritations occurred during long-term measurements. The electrodes were fabricated using a novel process for micro- and macrostructuring of different conductive polymer composites that is simple, cost efficient and upscalable. In conclusion, the biopotential electrodes presented here could enable preparation-free wearable medical and consumer devices for future health care and the Internet of Humans.

4. Experimental Section

Soft Porous Electrodes (Figure 1A): To produce electrically conductive polymers, uncured polymer (1:1 Ecoflex 00-30, Smooth-On) was mixed with 25 vol% silver microparticles (2–3.5 µm, Sigma-Aldrich) in a planetary mixer (Thinky ARE – 250). The resulting pasty composite was stencil printed through a laser-cut poly(methyl methacrylate) (PMMA) mask (A1) onto a flat substrate and cured in an oven at 80 °C (A2). A thin top layer of the composite with 30 vol% silver content was stencil printed on top to form a porous and highly conductive top layer. The electrode was released by removing the stencil mask (A3) and peeling from the substrate (A4).

Macropillar Electrodes (Figure 1B): The conductive base polymer was prepared as described above and was then stencil printed in a two-step process onto a flat substrate. First the macropillars were printed using a laser-cut mask of 2 mm thickness and second the base using a PMMA foil of 0.5 mm thickness (B2). Before peeling, the pillars were covered with highly conductive porous coating as described above (B3). The 12 resulting pillars were 1 mm in diameter (≈0.1 cm^2 total skin-contact area) and 2 mm high. The electrode was released by peeling from the substrate (B4).

Microstructured Electrodes (Figure 1C): Lift-off resist (1.5 µm LOR 10B, MicroChem) was spin-coated and cured on a silicon substrate and defines the height of the feet. Positive photoresist (10 µm PR AZ4562, MicroChem) was then spin-coated and cured on top of the LOR and defines the pillar height. The PR was subsequently exposed to UV in a mask aligner (MA6, Suess) to define the pillar diameter. Developer (400K, 1:3, Microchem) was used to generate the negative casting mold for micropillars and feet in a single step (C1). The developer first removed the exposed AZ4562 anisotropically and then etched LOR 10B isotropically. To produce the electrically conductive polymer, uncured polydimethylsiloxane (PDMS) (10:1 Sylgard 184, Dow Corning) is mixed 25 vol% silver microparticles of different size (AgSMP = 0.5–1 µm, Alfa Aesar, AgLMP = 2–3.5 µm, Sigma-Aldrich) in a planetary mixer. The resulting paste was stencil printed onto the microstructured wafer, degassed in vacuum, and cured in an oven at 80 °C (C2). The stencil mask was laser-cut from a thin foil (125 µm, Teonex Q51) and defined the geometry of the base. The electrodes were released by dissolving of LOR and PR in an acetone bath followed by isopropanol cleaning (C3, C4).

Impedance Measurements: The skin-contact impedance was measured with an impedance analyzer (PalmSens3) with a three-electrode setup. The electrode under test (i.e., the working electrode) was cleaned with ethanol before placing it on the skin of the lower forearm without skin preparation. Two clinical standard gold cup electrodes filled with electrolyte gel (Ten20 conductive, Neurodiagnostic Electrode Paste, Weaver, and company) serving as reference and counter electrodes were placed with a distance of 10 cm and 20 cm. The impedance was measured from 1 Hz to 1 kHz with 10 mV. All measurements were performed on the same day and on the same subject.

Adhesion Force Measurements: Perpendicular adhesion force was measured with a tensile testing machine (DO-FB0.5TS, Zwick/Roell). The polymer electrodes, without cover nor treatment, were attached with double sided tape to the force sensor. The forearm, without treatment, was placed underneath and the electrode brought into contact with 2 mm s^{-1} to an initial contact pressure of 0.64 N cm^{-2}. The electrode was pulled of the skin with 25 mm s^{-1}. The adhesion force was calculated as the difference between peak and baseline force value and normalized to the covered skin area.

Motion Artifact Measurements: To measure the effect of horizontal motion of the electrode on the ECG signal, a custom setup consisting of a two-axis moveable linear stage was used with active pressure control along the vertical axis. The electrode under test was placed on the lower arm, one counter electrode on the same arm with a distance of 8 cm and a second on the opposite arm. The electrodes were then connected to a biosensing platform (OpenBCI Cyton) for recording. The arm was placed on the linear stage for testing. For horizontal motion, the horizontal axis was actuated (± 7 mm), while the vertical axis maintained an actively controlled constant pressure (0.65 N cm^{-2}) on the electrode.

ECG Measurements: For ECG measurements during swimming, electrodes are placed according to the standard bipolar lead II. Clinical gel patch and dry electrodes were placed directly next to each other and the signals were recorded simultaneously. The data acquisition board (Olimexino-328 with Shield-EKG-EMG) was kept in a waterproof box and integrated into a garment worn by the test subject.

EEG Measurements: The macropillar electrodes were cleaned with ethanol and then positioned on the head on FP1 and O2 according to the 10–20 system. Clinical standard gold-cup electrodes on FP2 and O1 served as reference measurements, two more electrodes on the ears as bias and ground. Data of all channels were recorded in parallel using the OpenBCI platform. The power spectral density was calculated from 30s recordings for closed and open eyes. Informed signed consent was obtained from all subjects for measurement of skin-contact impedance, skin adhesion, motion artifacts, ECG, and EEG.

Statistical Analysis: Visualization and analyzes were done in Python using the seaborn and matplotlib library. Impedance measurements: all measurements are presented as mean with estimated confidence interval of 95% (bootstrapped with python seaborn library), $n = 3$.

Adhesion Force Measurements: Each boxplot shows the adhesive force distribution of 20 measurements, collected from 2 electrodes with 10 subsequent repetitions each. Motion artifact testing: Signals were filtered with a butterworth bandpass (0.5–120 Hz) and bandstop notch filter (49–51 Hz). RMS noise was calculated from 15 signal intervals (4 s each) from 3 different electrodes. Signal bandpowers were calculated by integrating the power spectral density. SNR of bandpower was calculated by dividing the signal bandpower by the noise bandpower.

Supporting Information

Supporting Information is available from the Wiley Online Library or from the author.

Acknowledgements

F.S. and M.T. contributed equally to this work. The authors would like to thank Nina Reinschmidt for testing of the electrodes in water and Andrea Fümm and Alfonso Blanco for design and packaging of the recording electronics. The authors further thank Dr. med. Christian Schmied from Uniklinik Zurich and Dr. med. Gabriele Wohlrab from Kinderspital Zurich for medical evaluation of the biopotential recordings. This project was funded by the Nanotera SpineRepair, BodyPoweredSense, and NextStep BioFlex programs of the Swiss National Science Foundation and ETH Zurich.

Conflict of Interest

Séverine Chardonnens and Simon Bachmann have co-founded IDUN Technologies AG which is aiming for commercialization of soft dry electrodes for non-invasive biopotential recordings in humans. All other authors report no conflicts of interest relevant to this article.

Keywords

adhesive, bioinspired, biopotential, epidermal electronics, stretchable electronics

Received: August 21, 2017
Revised: November 8, 2017
Published online: January 13, 2018

[1] H. Han, A. M. Reichmuth, A. F. Renz, F. Stauffer, M. Thielen, J. Voros, *Int. J. Autom. Smart Technol.* **2017**, *7*, 37.
[2] S. Yao, Y. Zhu, *JOM* **2016**, *68*, 1145.
[3] Y. M. Chi, T.-P. Jung, G. Cauwenberghs, *IEEE Rev. Biomed. Eng.* **2010**, *3*, 106.
[4] D.-H. Kim, J.-H. Ahn, W. M. Choi, H.-S. Kim, T.-H. Kim, J. Song, Y. Y. Huang, Z. Liu, C. Lu, J. A. Rogers, *Nature* **2008**, *320*, 507.
[5] K. I. Jang, H. N. Jung, J. W. Lee, S. Xu, Y. H. Liu, Y. Ma, J. W. Jeong, Y. M. Song, J. Kim, B. H. Kim, A. Banks, J. W. Kwak, Y. Yang, D. Shi, Z. Wei, X. Feng, U. Paik, Y. Huang, R. Ghaffari, J. A. Rogers, *Adv. Funct. Mater.* **2016**, *26*, 7281.
[6] Y. H. Chen, M. Op de Beeck, L. Vanderheyden, E. Carrette, V. Mihajlović, K. Vanstreels, B. Grundlehner, S. Gadeyne, P. Boon, C. van Hoof, *Sensors* **2014**, *14*, 23758.
[7] P. C. P. Watts, S. J. Henley, E. Mendoza, S. R. P. Silva, J. K. Irvine, E. T. McAdams, *Nanotechnology* **2007**, *18*, 205502.
[8] B. A. Reyes, H. F. Posada-Quintero, J. R. Bales, A. L. Clement, G. D. Pins, A. Swiston, J. Riistama, J. P. Florian, B. Shykoff, M. Qin, K. H. Chon, S. S. Member, H. F. Posada-Quintero, S. S. Member, J. R. Bales, A. L. Clement, G. D. Pins, A. Swiston, J. Riistama, J. P. Florian, B. Shykoff, M. Qin, K. H. Chon, S. S. Member, *IEEE Trans. Biomed. Eng.* **2014**, *61*, 1863.
[9] T. Thap, K.-H. Yoon, J. Lee, *Sensors* **2016**, *16*, 542.
[10] S. M. Lee, H. J. Byeon, J. H. Lee, D. H. Baek, K. H. Lee, J. S. Hong, S.-H. Lee, *Sci. Rep.* **2014**, *4*, 1200.
[11] A. C. Myers, H. Huang, Y. Zhu, *RSC Adv.* **2015**, *5*, 11627.
[12] T. C. Ferree, P. Luu, G. S. Russel, D. M. Tucker, *Clin. Neurophysiol.* **2001**, *112*, 536.
[13] M. Weder, D. Hegemann, M. Amberg, M. Hess, L. F. Boesel, R. Abächerli, V. R. Meyer, R. M. Rossi, *Sensors* **2015**, *15*, 1750.
[14] T. Kim, J. Park, J. Sohn, D. Cho, S. Jeon, *ACS Nano* **2016**, *10*, 4770.
[15] C. Greiner, A. Del Campo, E. Arzt, *Langmuir* **2007**, *23*, 3495.
[16] R. Spolenak, S. Gorb, H. Gao, E. Arzt, *Proc. R. Soc. London, Ser. A* **2005**, *461*, 305.
[17] W. G. Bae, D. Kim, M. K. Kwak, L. Ha, S. M. Kang, K. Y. Suh, *Adv. Healthcare Mater.* **2013**, *2*, 109.
[18] A. Larmagnac, S. Eggenberger, H. Janossy, J. Vörös, *Sci. Rep.* **2014**, *4*, 7254.
[19] L. Tchvialeva, H. Zeng, I. Markhvida, D. I. McLean, H. Lui, T. K. Lee, in *New Dev. Biomed. Eng.*, InTech, Vienna, Austria **2010**, https://doi.org/10.5772/7611.
[20] M. Kamperman, E. Kroner, A. Del Campo, R. M. McMeeking, E. Arzt, *Adv. Eng. Mater.* **2010**, *12*, 335.
[21] G. Carbone, E. Pierro, S. N. Gorb, *Soft Matter* **2011**, *7*, 5545.